Ab initio calculations of structural and electronic properties of CdTe clusters

Somesh Kr. Bhattacharya* and Anjali Kshirsagar†
Department of Physics, University of Pune, Pune 411 007, India
(Received 18 April 2006; revised manuscript received 6 November 2006; published 2 January 2007)

We present results of a study on small stoichiometric Cd_nTe_n $(1 \leqslant n \leqslant 6)$ clusters and a few nonstoichiometric Cd_mTe_n $[(m,n=1,4,13,16,19);\ (m \neq n)]$ clusters using the density functional formalism and projector augmented wave method within the generalized gradient approximation. Structural properties viz. geometry, bond length, symmetry, and electronic properties such as the highest occupied molecular orbital (HUMO) and lowest unoccupied molecular orbital (LUMO) gap, binding energy, ionization potential, nature of bonding, etc., have been analyzed. The initial geometries of nonstoichiometric clusters were considered as fragments of the bulk with T_d symmetry. It was observed that upon relaxation, the symmetry changes for the Cd-rich clusters whereas the Te-rich clusters retain their symmetry. It may be mentioned that the Te p lone pair repulsion drives the Te atoms to the surface and renders stability to the clusters. The Cd-rich clusters develop a HOMO-LUMO gap due to relaxation whereas there is no considerable change in the HOMO-LUMO gap of the Te-rich clusters. Thus, the symmetry of a cluster seems to be an important factor in determining the HOMO-LUMO gap. To render the surface of a quantum dot inert, passivation is essential. In the present work, we have passivated the nonstoichiometric clusters using fictitious "hydrogen like" pseudoatoms. It was observed that passivation removed the states in the HOMO-LUMO gap region resulting in widening of the gap. The symmetry of the clusters, however, remains unchanged upon passivation.

DOI: 10.1103/PhysRevB.75.035402 PACS number(s): 61.46.−w, 61.46.Df, 71.15.Mb, 73.22.−f

I. INTRODUCTION

Semiconductor nanoparticles or quantum dots (QDs), in particular of II-VI materials, have received tremendous attention during the last two decades owing to their unusual physical properties and wide range of applications.[1] A systematic study of QDs is useful to understand the evolution of their physical and chemical properties with size. Moving from a molecule to bulk, one can observe a range of variation of fundamental properties. This size-dependent effect, however, is most significant for small-sized clusters and is attributed to different geometry of the clusters in comparison to the bulk. Quantum confinement of electronic states and large surface to volume ratio together modify the properties of these clusters. In bare clusters, unsaturated bonds lead to peculiar structural and electronic properties such as surface reconstruction, formation of new cleavage planes, etc.

The differences in the structural properties also affect the electronic properties of the QDs. In bulk systems one observes quasicontinuous electronic levels forming bands whereas in clusters the electronic levels are discrete. Apart from the structural and electronic properties, other properties such as the thermodynamic and optical properties too differ significantly for clusters as compared to bulk.[2,3]

Among the II-VI semiconductors, CdX (X=S,Se,Te) systems have potential applications in optical and optoelectronic devices. CdTe nanoclusters, in particular, are used in optical sensors. Multilayered CdTe thin films with poly (diallyl dimethyl ammonium chloride) are electroactive and photoactive and hence are used in neuroprosthetic devices.[4] Self-assembled CdTe nanodots have high efficiency in terms of photoluminescence and hence are appropriate candidates for the purpose of making LEDs. CdTe and Au nanohybrid materials have photoluminescence variation depending upon environmental conditions such as temperature, ionic strength, and solvents, and hence are used as biosensors.[5]

We present density functional theory (DFT) based calculations for some stoichiometric, Cd_nTe_n $(1 \leqslant n \leqslant 6)$, and a few nonstoichiometric Cd_mTe_n $(m,n=1,4,13,16,19)$ $(m \neq n)$ clusters. Both Cd and Te in bulk phase exist in hexagonal structure with c/a ratios of 1.89 and 1.33, respectively,[6] whereas CdTe in bulk phase has lattice constant a=6.48 Å in zinc-blende (ZB) structure and a=4.57 Å and c=7.47 Å in wurtzite structure. In bulk, the wurtzite (W) structure is higher in energy by 9 meV per Cd-Te pair than the ZB structure.[7] CdTe has a calculated direct band gap of 1.59 eV at the Γ point.[8]

The study of small clusters is challenging due to lack of experimental structural information and increased degree of freedom. Very small clusters (containing up to 8–10 atoms) exhibit symmetry and have only a few possible geometries. On the other hand, nonstoichiometric clusters can be considered as fragments of bulk, possessing the same structural symmetry as that of the bulk.[9] To the best of our knowledge, so far no *ab initio* calculations have been reported on CdTe QDs. Structural, electronic, and optical properties of II-VI semiconductor nanoclusters have been studied using a variety of methods based on *ab initio* DFT, quantum chemistry methods such as Hartree-Fock, Gaussian, etc., and approximate methods such as the tight-binding method.[10–13]

An important step in modeling the electronic structure of QDs is passivation. Bare clusters have dangling bonds at their surfaces. These unsaturated bonds alter the chemical and electronic properties of the QDs and therefore have to be satisfied. Recently several methods have been proposed for passivation.[14–16] In the present work, we use the recipe for passivation as prescribed by Chelikowsky *et al.*[17] Passivation provides a handle to compare theoretical results with experiments for large clusters.

II. METHODOLOGY AND COMPUTATIONAL DETAILS

The first step for calculating the cluster properties is the determination of the lowest energy configuration. Existence of several configurations with varying coordination and multiple minima in the potential energy surface enormously complicates the problem, making it almost impossible to decide the lowest energy configuration for clusters by direct calculation, especially for larger clusters.

Present work is based on the Kohn-Sham density functional framework.[18] The electronic structure is calculated self-consistently using projector augmented wave (PAW) method[19] as implemented in the VASP package[20] within the framework of GGA instead of the Vanderbilt ultrasoft (US) pseudopotential[21] (PP) as it provides better first principle simulations in comparison to US-PP.[19] In pseudopotential methods, the effect of core electrons and nuclei is replaced by an effective ionic potential and only the valence electrons, which are directly involved in chemical bonding, are considered. The valence electron configurations used for Cd and Te are $5s^2 4d^{10}$ and $5s^2 5p^4$, respectively. The $4d$ levels in Te atom are well separated from the $5s$ levels and hence can be included in the core.

Various parametrizations have been used for different exchange-correlation potentials[22] in the DFT formalism in the literature. In this work we have used Perdew-Berke-Ernzerhof (PBE) exchange correlation[23] for our calculations as it is known to improve total energy and molecule atomization energy and therefore the electronic properties, as compared to PW91 (Ref. 24) and the results agree with those of the experiments very well.

Two different categories of clusters (different size regime and stoichiometry) have been studied in this work as discussed earlier. The geometry of small clusters varies significantly from the bulk. We have chosen several possible geometries by exploiting the symmetry considerations and by exchanging the positions of cationic and anionic atoms. CdTe in bulk has ZB structure with T_d symmetry. Therefore, for nonstoichiometric clusters Cd_mTe_n $(m \neq n)$, the initial geometry was considered as a fragment of the ZB structure. Six clusters, in particular, have been studied viz. Cd_1Te_4, Cd_4Te_1, $Cd_{13}Te_{16}$, $Cd_{16}Te_{13}$, $Cd_{16}Te_{19}$, and $Cd_{19}Te_{16}$. Each geometry is allowed to relax and the local minimum is found using conjugate gradient (CG) method as implemented via Kosugi algorithm[25] (special Davidson block iteration scheme).

The size of the basis set was optimized by varying the plane wave cut off to obtain total energy convergence. The plane wave cut off was set to 274.3 eV for both the types of clusters. Calculations are done in a supercell geometry with the cluster placed at the center of the cell. Size of the supercell should be large enough to mimic free cluster geometry with enough vacuum region around each cluster. The supercell size was optimized with respect to the total energy convergence.

The size of the supercell was chosen to be $a=20$ Å for Cd_1Te_4 and Cd_4Te_1 which is sufficiently large to minimize intercluster interactions. We have used a supercell with $a=30$ Å for the remaining four nonstoichiometric clusters and $a=25$ Å for the small stoichiometric clusters Cd_nTe_n $(1 \leqslant n \leqslant 6)$. The sizes of the supercells considered for our calculations guarantee that the charge densities are confined well within the box with sufficient vacuum region between the cluster and its images, thereby removing any inter-cluster interactions. In all the structure minimizations, the force and energy convergence obtained was $\sim 10^{-3}$ eV/Å and $\sim 10^{-4}$ eV, respectively.

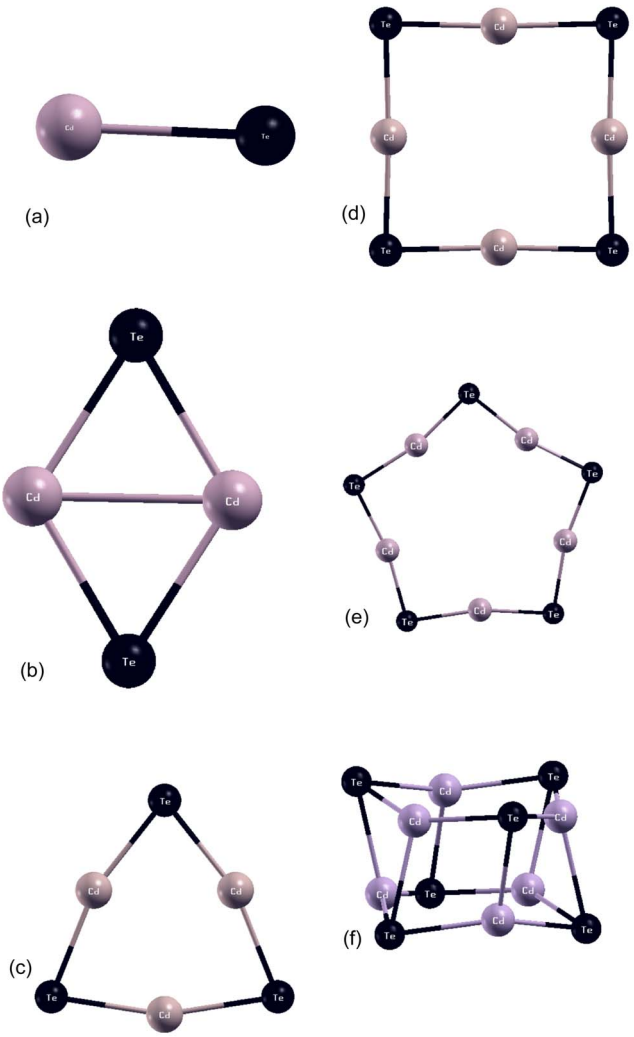

FIG. 1. (Color online) Lowest energy structures (LES) of Cd_nTe_n clusters for $(1 \leqslant n \leqslant 6)$. Black atoms are Te atoms.

To study the effect of passivation, we have passivated the nonstoichiometric clusters with fictitious hydrogen (H^*) atoms.[17] Two types of fictitious hydrogen atoms were used to passivate the dangling bonds. One species has nuclear charge of $(1+\eta)$ and a valence electron charge of $-(1+\eta)$, where η is a positive number. These atoms are bonded to Cd. The other species, having nuclear charge of $(1-\eta)$ and valence electron charge of $-(1-\eta)$, is bonded to Te. It has been observed that the highest occupied molecular orbital (HOMO) - lowest unoccupied molecular orbital (LUMO) gap opens up maximum at $\eta=0.5$ for these clusters.

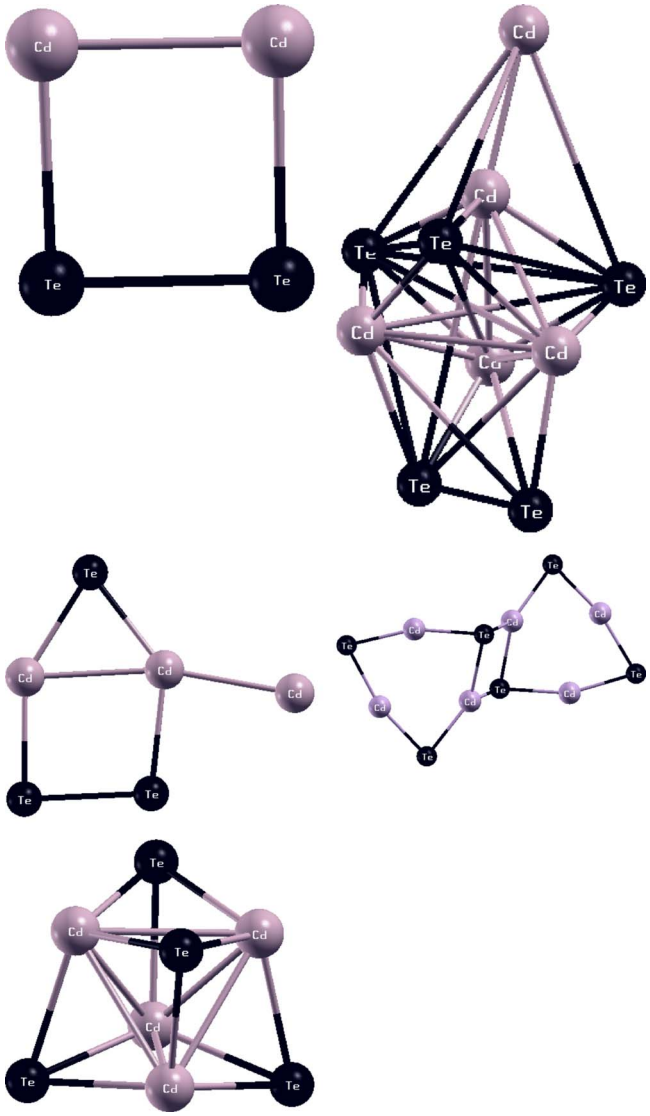

FIG. 2. (Color online) Geometries of the first local minima of Cd_nTe_n for $(2 \leqslant n \leqslant 6)$. Black atoms are Te atoms.

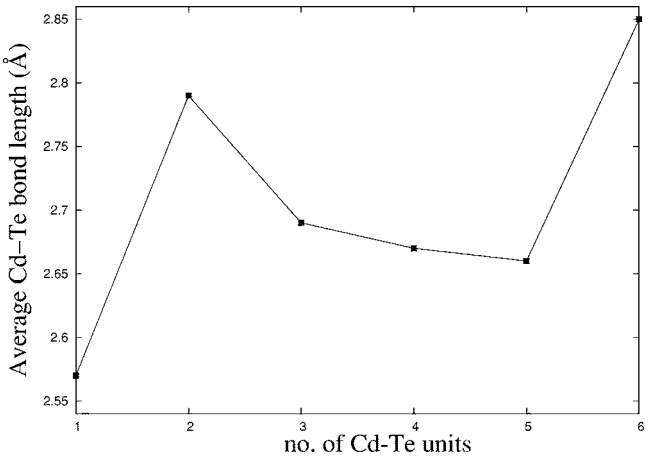

FIG. 3. Average Cd-Te bond length in Å vs number of Cd-Te units.

III. RESULTS AND DISCUSSIONS

A. Structural properties of Cd_nTe_n

The geometries for lowest energy called the lowest energy structures (LES) of Cd_nTe_n obtained by CG are shown in Fig. 1 and those for first local minima structures (FLMS) in Fig. 2. It is interesting to note that for all the calculated lowest energy structures, the chalcogenide atoms are at the peripheral positions. This is a direct consequence of Coulomb repulsion between the lone-pair electrons situated on the chalcogenide atoms which is minimized by pushing these atoms towards the peripheral position. As expected, the ground state structures of these CdTe clusters do not resemble the bulk phase.

CdTe dimer is a linear molecule with bond length of 2.57 Å and belongs to $C_{\infty v}$ point group. For Cd_2Te_2, Cd_3Te_3, Cd_4Te_4, Cd_5Te_5, and Cd_6Te_6, there are two possible lowest energy configurations within the energy difference of ~0.11, ~0.22, ~0.04, ~0.05, and ~0.16 eV per atom, respectively. Except for Cd_6Te_6, the lowest energy geometry is a planar ringlike structure. Cd_2Te_2 has LES as the rhombic structure and a square planar structure as FLMS. The LES and FLMS belong to D_{2h} and C_{2v} point groups, respectively. Cd_3Te_3 has triangular structure (D_{3h} point group) as LES configuration and another planar structure (C_s point group) as the FLMS. No three-dimensional (3D) stable geometry is obtained for $n=2,3$. For Cd_4Te_4, the square planar (D_{4h} point group) geometry is obtained for LES and 3D tetrahedral structure (T_d point group) as FLMS. Cd_5Te_5 is a planar pentagon (C_s point group) for LES and a nonsymmetric 3D structure for FLMS. A transition from planar LES to 3D LES occurs for $n=6$. For Cd_6Te_6, both the LES and FLMS are 3D structures. The LES is a cage structure with C_1 point group symmetry. This is attributed, as explained later, to the tendency of achieving higher coordination without putting too much strain on the bond angles. All the atoms in planar clusters, except for the FLMS of Cd_3Te_3, have coordination 2.

The geometries obtained for the CdTe clusters are quite similar to those of corresponding CdS and CdSe clusters up to $n=4$.[26] However, the geometries of Cd_5Te_5 and Cd_6Te_6 are very different from the CdS and CdSe counterparts.[26] This difference may be attributed to the fact that (i) we have used GGA for the exchange correlation potential whereas calculations are done in Ref. 26 with LDA and (ii) we have included $4d$ of Cd in the valence configuration whereas in Ref. 26 so called "partial core correction" is used. It may be mentioned that Wei and Zunger[27] have emphasized the importance of including d levels of the cations in the valence configuration for determination of electronic structure of bulk II-VI semiconductors.

The ionic and covalent radii increase in going from S to Se and then to Te whereas electronegativity and ionization energies decrease.These factors play an important role in determining the structures of heteronuclear clusters. We have, therefore, compared the structures of Cd_nTe_n clusters with those of Zn_nS_n clusters.[28] We found that the LES and FLMS for both ZnS and CdTe clusters match up to ten atoms. This similarity may be due to the fact that the difference in properties such as covalent and ionic radii, electronegativity, and ionization energies between Cd and Te are similar to those between Zn and S.

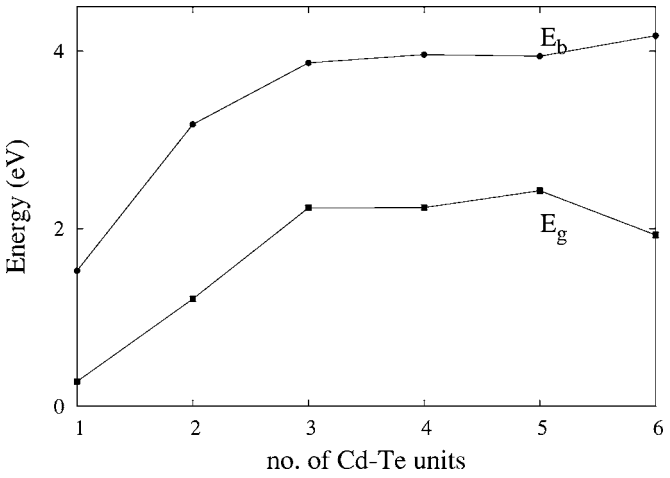

FIG. 4. HOMO-LUMO gap E_g and binding energy E_b (in eV) vs number of Cd-Te units.

As we move from planar to 3D structure the coordination of atoms increases from 2 to 3 and in some cases to 4 also. A comparison of Cd_nTe_n clusters with Cd_n (Ref. 29) shows that three dimensional structures are more favorable in pure Cd clusters as compared to CdTe clusters where planar structure is favored even for a ten atom cluster.

Figure 3 shows the variation of average Cd-Te bond length with the number of Cd-Te pairs (n) in the clusters. The near neighbor (NN) distance for CdTe bulk is 2.81 Å. As evident from Fig. 3, these clusters have an average bond length less than the NN distance in bulk. This is due to incomplete coordination in these clusters on account of very small number of atoms. The bond length of CdTe dimer is the smallest. In fact, the smallest Cd-Te bond length remains almost constant in these clusters for $n=3-6$ (not shown in figure). The average Cd-Te bond length shrinks with increasing n in planar structures ($n=2-5$) and increases in going from planar to 3D structures.

Surface studies[30] on heteropolar covalent and ionic semiconductors have identified quantum mechanical electron-electron Coulomb repulsion, hybridization effects, and classical Coulomb attraction between anion and cation as competing factors in deciding the stability of the surface. The last factor seems to be more important with only three neighbors for atoms on the surface. Optimum energy gain is achieved when the distance between anion and cation is as small as possible. Thus shorter bonds are more ionic in nature. We therefore expect that CdTe dimer will have more ionic character as compared to other clusters. In Cd_2Te_2, a covalent bond exists between two Cd atoms which accounts for an increase in average Cd-Te bond length. As explained later from the charge density plots, there are no covalent bonds between two similar atoms (either Cd-Cd or Te-Te) in other planar structures ($n=3-5$). Therefore, the average Cd-Te bond length is smaller in these clusters. The LES for Cd_6Te_6 is similar to a fragment of the bulk W CdTe. The surface atoms are relaxed due to incomplete coordination. Hence the average Cd-Te bond length is close to the bulk value.

Cd-Cd bond length in Cd_2Te_2 is smaller (2.87 Å) than in Cd dimer (3.47 Å). The average Cd-Cd bond length is same in Cd_3Te_3 and Cd_3. However, it is larger in Cd_nTe_n as compared to Cd_n for $4 \leqslant n \leqslant 6$. In contrast, average Te-Te bond length is significantly larger in CdTe clusters in comparison to pure Te clusters[31] as expected due to lone pair repulsion effective in heteronuclear clusters. Also it does not appreciably change with n.

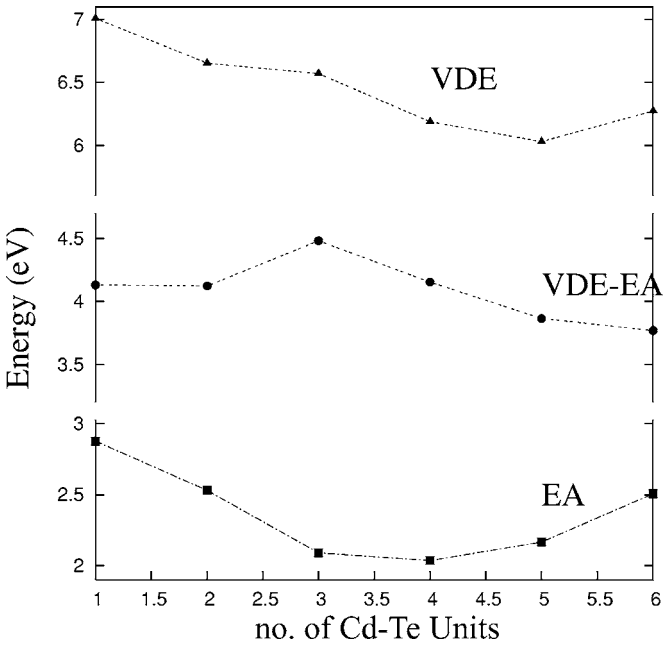

FIG. 5. Vertical detachment energy (VDE), electron affinity (EA), and (VDE-EA) (in eV) vs number of Cd-Te units.

Average Te-Cd-Te bond angle increases from 107.2° in Cd_2Te_2 to nearly 180° in Cd_4Te_4. The angle further opens up in Cd_5Te_5. In Cd_6Te_6, all the Te-Cd-Te angles are smaller than linear angle as a consequence of 3D structure. Thus we see that smaller clusters have a tendency to form linear Te-Cd-Te bonds resulting in planar structures with coordination of 2 and as higher coordination number takes over, a transition from planar to three dimensional structure results for stable geometry. All the clusters are found to be stable against fragmentation into smaller clusters.

B. Electronic properties of Cd_nTe_n

Figure 4 depicts variation in the energy gap between HOMO and LUMO (E_g) and the binding energy (E_b) per Cd-Te unit [defined in Eq. (1)] with the number of Cd-Te units in the cluster.

$$E_b = (n\{E[\mathrm{Cd}] + E[\mathrm{Te}]\} - E[\mathrm{Cd}_n\mathrm{Te}_n])/n, \qquad (1)$$

where $E[A]$ represents the total energy of system A.

The corresponding two curves for CdS and CdSe show similar trends[26] and the authors claim to infer the stability of clusters from the maximum in these curves. Variation of E_g suggests that Cd_5Te_5 is more stable compared to its neighbors. However, the E_b curve indicates that larger n clusters may be more stable. It may be mentioned that the E_b curve does not show saturation with n up to $n=6$.

The vertical detachment energy (VDE) and electron affinity (EA), shown in Fig. 5, are calculated using Eqs. (2) and

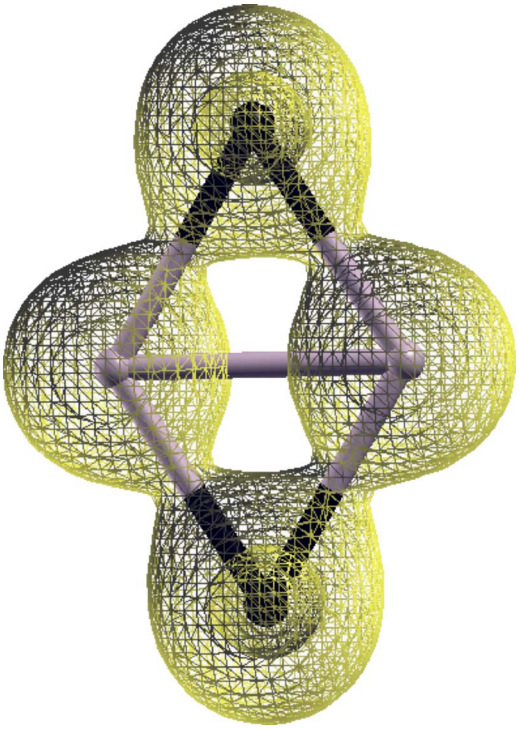

FIG. 6. (Color online) Charge density isosurface for Cd_2Te_2. The Grey atoms are Cd and black atoms are Te.

(3) by performing two self-consistent calculations for different electronic systems without allowing any change in the lowest energy geometry of the neutral cluster:

$$\mathrm{VDE}[\mathrm{Cd}_n\mathrm{Te}_n] = E[(\mathrm{Cd}_n\mathrm{Te}_n)^+] - E[\mathrm{Cd}_n\mathrm{Te}_n], \quad (2)$$

$$EA[\mathrm{Cd}_n\mathrm{Te}_n] = E[\mathrm{Cd}_n\mathrm{Te}_n] - E[(\mathrm{Cd}_n\mathrm{Te}_n)^-]. \quad (3)$$

VDE monotonically decreases with n up to $n=5$, indicating that it is easier to ionize larger clusters. However, $n=6$, being a bulk fragment, is stable with respect to ionization. EA shows a dip near $n=4$ implying that Cd_4Te_4 favors addition of electron compared to its neighbors. VDE-EA is physically a more meaningful quantity. It is a measure of stability of clusters with respect to ionization. The VDE-EA curve in Fig. 5 shows that $n=3$ cluster is the most stable cluster with respect to addition or removal of an electron.

The nature of bonding is another important parameter in analyzing the electronic properties. In bulk CdTe, the bonding is largely covalent as the atomic number and hence the atomic radii for Cd and Te are very close. As a result, the Coulombic forces between the two species are balanced very well. However, due to the difference in electronegativity of Cd and Te, the bonding has some ionic character even in the bulk.

To discuss the nature of bonding, we show total charge density isosurface plot for the Cd_2Te_2 cluster in Fig. 6 revealing covalent bonding. Similar charge density distributions are seen for other clusters too. No Cd-Cd or Te-Te near neighbor bonds are seen to be formed for clusters with $n>2$. The charge density plots for CdS and CdSe (Ref. 26) show that the bonding is not purely covalent; it has some ionic character. Ionicity in bonding is more in CdS than in CdSe because of smaller atomic radius of sulfur than selenium. Ionicity is thus expected to be still smaller in CdTe.

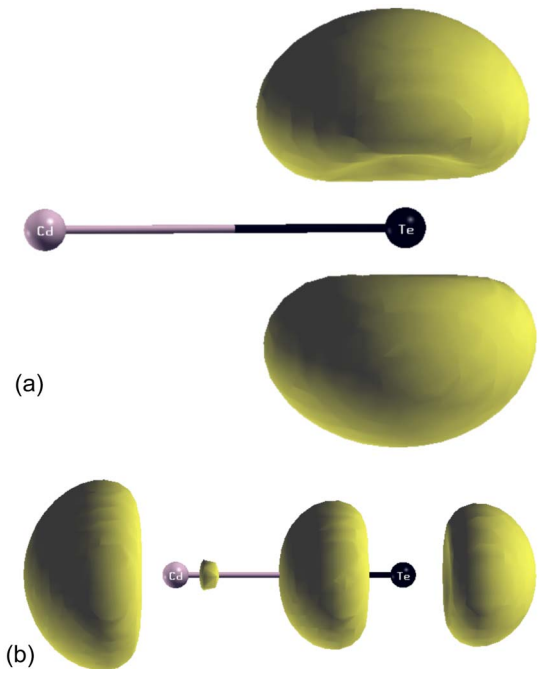

FIG. 7. (Color online) Isosurface plots of partial charge density of (a) HOMO, (b) LUMO for CdTe dimer.

An analysis of charge inside atomic spheres with covalent radii, shows that the distribution of charge in the Cd and Te spheres is almost same for planar structures as n changes from 3 to 5. This charge analysis was also compared with the Mulliken, Lowdin, and Hirshfeld charges obtained from GAUSSIAN-98 package[32] for the LES for these clusters.

A more detailed information regarding the bonding in these clusters can be obtained from the partial charge density plots associated with specific molecular orbitals (MOs) in these clusters. It is evident from Fig. 7(a) that the HOMO consists of purely Te p. In the LUMO, Cd s and p hybridize to give a sp-hybrid orbital which in turn forms a σ bond with the Te p orbital as seen in Fig. 7(b). Similar trends are seen for the partial charge density isosurface plots for HOMO and LUMO of Cd_4Te_4 as shown in Figs. 8(a) and 8(b). Figure 8(b) shows delocalization of the charge density in the central region of the cluster indicating a semimetallic character in the bonding. Such systems will favor electron addition as is also evident from the EA curve in Fig. 5. For other clusters the partial charge densities for HOMO and LUMO have similar natures. As seen from the MO charge distribution of HOMO, as one goes from $n=2$ to $n=5$, an enhancement in delocalization results accounting for a steady decrease in the VDE as shown in Fig. 5.

In Fig. 9 we show the one-electron energies for all the CdTe clusters and the atomic levels of Cd and Te. The Cd s and the Te p levels lie in the same energy window in the atomic case. Consequently, an intermixing of these orbitals occurs in the clusters. A comparison of the one-electron energies with the fat band analysis of the CdTe bulk band structure (not shown here) using full potential linear augmented

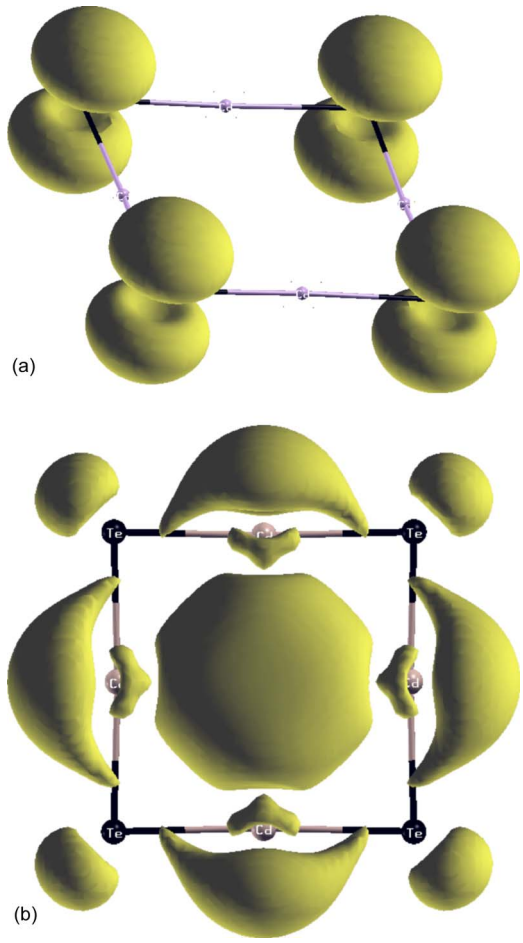

FIG. 8. (Color online) Isosurface plots of partial charge density of (a) HOMO and (b) LUMO for Cd_4Te_4.

plane wave method[33] along with comparisons of corresponding partial density of states (DOS) and charge distribution reveals that nature of HOMO is similar to the nature of top of valence band and that of LUMO is similar to bottom of the conduction band. Thus it seems that the bulk type hybridization of the orbitals is retained in clusters. The movement of the HOMO and LUMO in these small clusters is quite interesting. As the cluster size increases, the HOMO moves downward whereas the LUMO moves upward resulting in widening of the HOMO-LUMO gap. However, this shift is not uniform. The HOMO moves downward slowly as compared to the LUMO which moves upward rapidly. But for Cd_6Te_6, the HOMO shifts slightly upward and the LUMO shifts downward resulting in a smaller HOMO-LUMO gap as a consequence of planar to 3D transition in geometry.

C. Properties of Cd_mTe_n clusters

CdTe, with many other II-VI semiconductors, has ZB and W phases possible in bulk. There are also reports of size induced phase transitions in CdS (Ref. 34) nanoparticles. The first coordination for central atom is identical in ZB and W phases. If we consider the trigonal axis [111] in ZB and [001] in W then three near neighbors are identical.

We have, therefore, performed calculations for two small and four larger nonstoichiometric CdTe clusters viz. Cd_1Te_4 (central Cd+1 neighboring shell), $Cd_{13}Te_{16}$ (central atom +3 neighboring shells), $Cd_{16}Te_{19}$ (central atom + 4 neighboring shells), Cd_4Te_1, $Cd_{16}Te_{13}$, and $Cd_{19}Te_{16}$. The later three geometries are obtained from the former three by interchanging the positions of Cd and Te atoms. These clusters have been considered as fragments of the bulk and hence their initial symmetry is T_d as shown in Figs. 10(a) and 11(a).

Cd_1Te_4 has a central Cd atom and four neightboring Te atoms as shown in Fig. 12(a). Relaxation destroys the initial T_d symmetry and the cluster attains a lower symmetry structure. The HOMO-LUMO gap is 1.16 eV and the binding energy is 2.25 eV. In contrast, Cd_4Te_1 is not at all stable. Relaxation fragments the cluster separating two Cd atoms from the initial unit.

$Cd_{13}Te_{16}$ has a central Cd atom and the side views of its initial and relaxed structure are shown in Figs. 11(a) and 11(b), respectively. Figure 11(c) shows the side view of relaxed structure of $Cd_{16}Te_{13}$ which has a central Te atom.

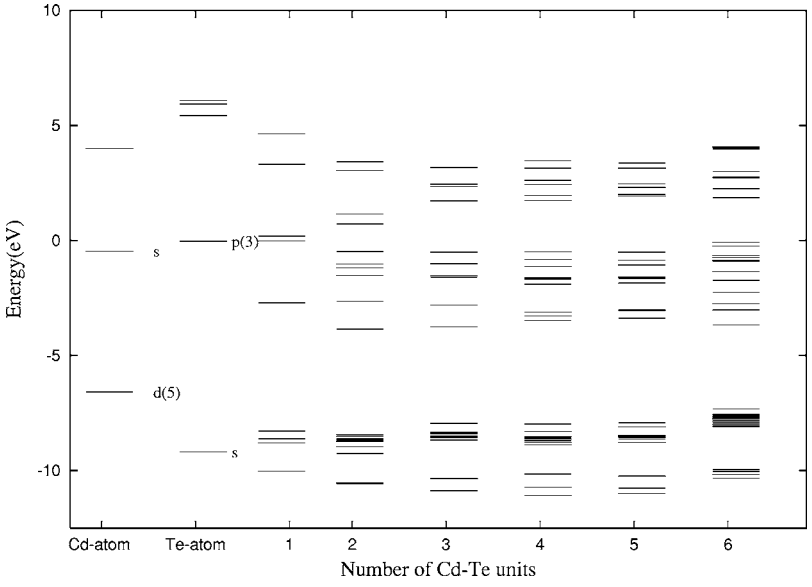

FIG. 9. Energy level diagram of CdTe clusters. Energy zero represents the Fermi energy for respective clusters.

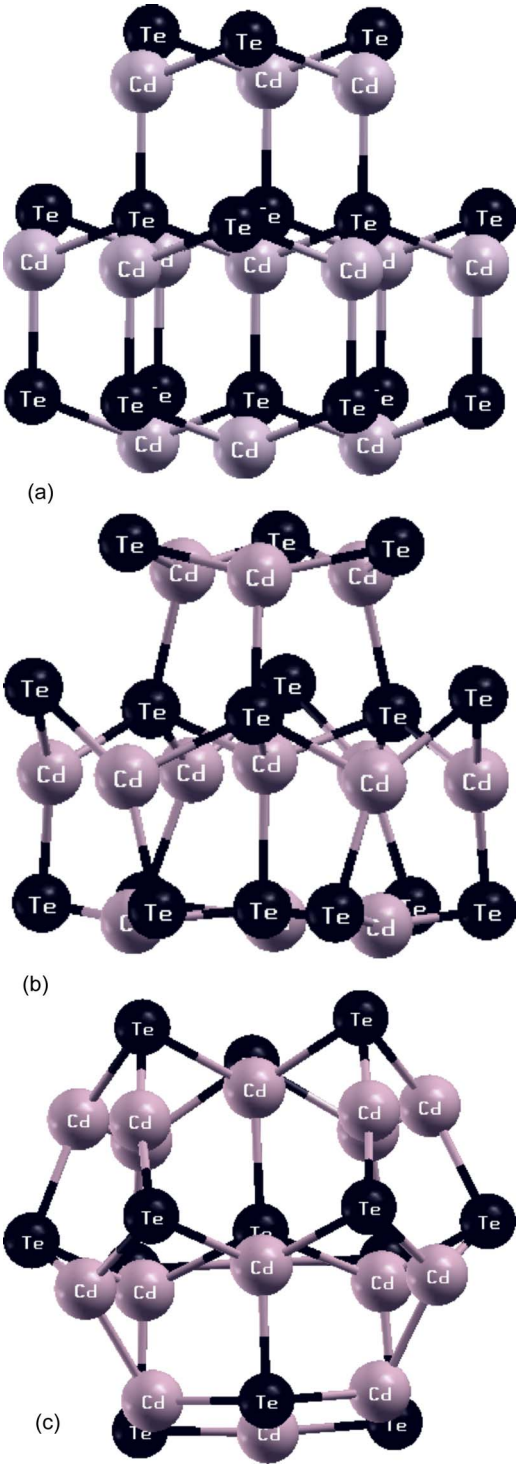

FIG. 10. (Color online) Side view of the initial and relaxed geometries. Black atoms are Te atoms. (a) $Cd_{13}Te_{16}$: initial, (b) $Cd_{13}Te_{16}$: relaxed, (c) $Cd_{16}Te_{13}$: relaxed.

During relaxation the central Te atom pushes the neighboring Cd atoms outward. Figure 12 shows the top views of initial geometry for $Cd_{16}Te_{19}$ (a) and the relaxed geometries for $Cd_{16}Te_{19}$ (b) and $Cd_{19}Te_{16}$ (c). It is found that upon relaxation only the Te-rich clusters retain their T_d symmetry whereas the Cd-rich clusters attain lower symmetry structures.

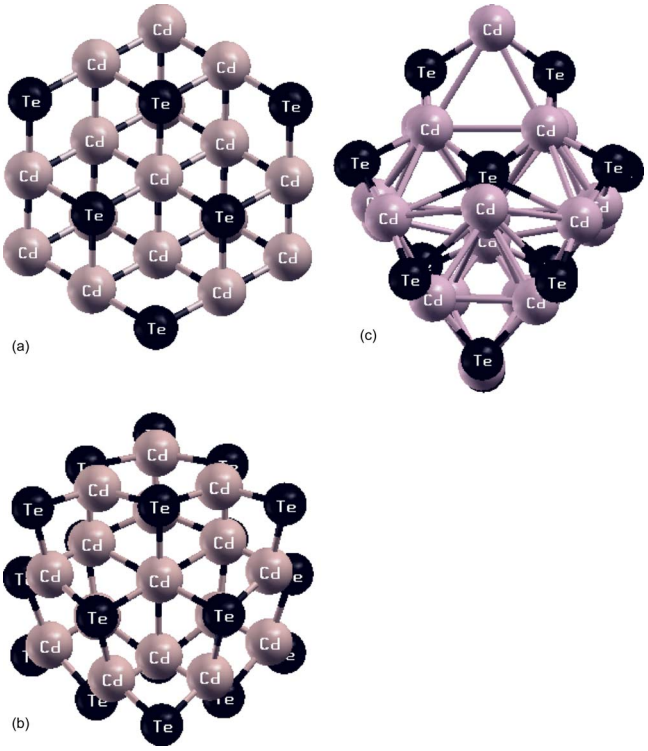

FIG. 11. (Color online) Top view of the initial and relaxed geometries. Black atoms are Te atoms. (a) $Cd_{16}Te_{19}$: initial, (b) $Cd_{16}Te_{19}$: relaxed, (c) $Cd_{19}Te_{16}$: relaxed.

We summarize in Table I some of the structural and electronic properties of Cd_mTe_n clusters. It may be mentioned that the binding energy of CdTe dimer is 0.76 eV/atom whereas the cohesive energy of CdTe bulk is 4.9 eV.

A comparison of the binding energies of the above clusters indicates that $Cd_{13}Te_{16}$ and $Cd_{16}Te_{19}$ are more stable than $Cd_{16}Te_{13}$ and $Cd_{19}Te_{16}$. In the former group the Te atoms are on the surface and hence these structures are energetically favored as discussed earlier for smaller clusters. For the Te-rich clusters, the relaxation is not strong enough to break their initial T_d symmetry. On the other hand, the Cd-rich clusters, being weakly bound, go to lower symmetry structures upon relaxation. The binding energy per atom for Cd_mTe_n clusters is higher than the corresponding Hg_mTe_n clusters.[9] This is attributed to symmetry allowed *pd* interactions. The *d* levels of Hg are closer than those of Cd to the *p* levels of Te. Therefore *pd*-repulsion induced bond weakening is more in HgTe than in CdTe clusters resulting in a reduction of binding energy.

A very interesting feature observed in the Cd-rich clusters is Jahn-Teller distortion. The initial HOMO-LUMO gap for $Cd_{16}Te_{13}$ and $Cd_{19}Te_{16}$ is nearly zero. But upon relaxation, they attain an appreciable HOMO-LUMO gap. This is a clear indication that the energy levels which are nearly degenerate in the initial structure have moved apart during relaxation. Thus, relaxation has destroyed the symmetry, resulting in lifting of degeneracy. On the other hand for the Te-rich clusters, the HOMO and LUMO are not degenerate (though close to each other) and thus there is no Jahn-Teller distortion. Similar trend has also been observed in nonstoichiometric

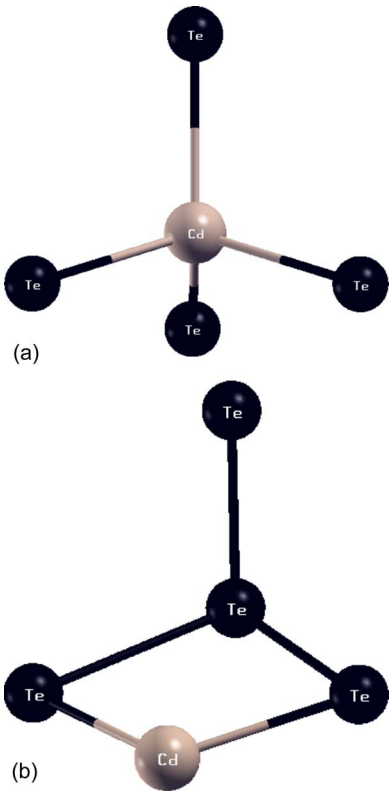

FIG. 12. (Color online) (a) Initial and (b) relaxed geometries of Cd_1Te_4. Black atoms are Te atoms.

HgTe clusters.[9] The Hg-rich clusters, upon relaxation, lose their initial T_d symmetry. As a result, they attain a definite bandgap and a semimetal to semiconductor transition is observed. Dalpian *et al.* have shown that symmetry is an important parameter in deciding the properties of nanoclusters.[35]

We passivated three specific clusters viz. Cd_1Te_4, Cd_4Te_1, and $Cd_{13}Te_{16}$ to see the effect of passivation by using 12 fictitious hydrogen (H^*) atoms for Cd_1Te_4 and Cd_4Te_1 and 30 for $Cd_{13}Te_{16}$. All the clusters retain their initial T_d symmetry. The observation is in contrast to the relaxation of bare five atom clusters [e.g., compare Figs. 10(b) and 13(a)]. On the other hand, the larger cluster geometry is almost the same for bare and passivated clusters [Figs. 11(b) and 13(c)] in agreement with Puzder *et al.*[36] The structural and electronic properties of these passivated clusters are summarized in Table II.

TABLE I. Summary of structural and electronic properties of relaxed $Cd_mTe_n(m \neq n)$ clusters. PG is the observed point group symmetry, BE is binding energy expressed in (eV/atom), l is average Cd-Te bond length in Å, θ is the Y-X-Y bond angle at the central atom X of the cluster, and E_g is the HOMO-LUMO gap in eV.

Clusters	PG	BE	l	θ	E_g
$Cd_{13}Te_{16}$	T_d	2.13	2.81	109.47°	0.195
$Cd_{16}Te_{13}$	C_{3v}	1.95	2.84	109.48°	0.659
$Cd_{16}Te_{19}$	T_d	2.14	2.82	109.47°	0.088
$Cd_{19}Te_{16}$	C_1	1.95	2.81	91.31°	0.964

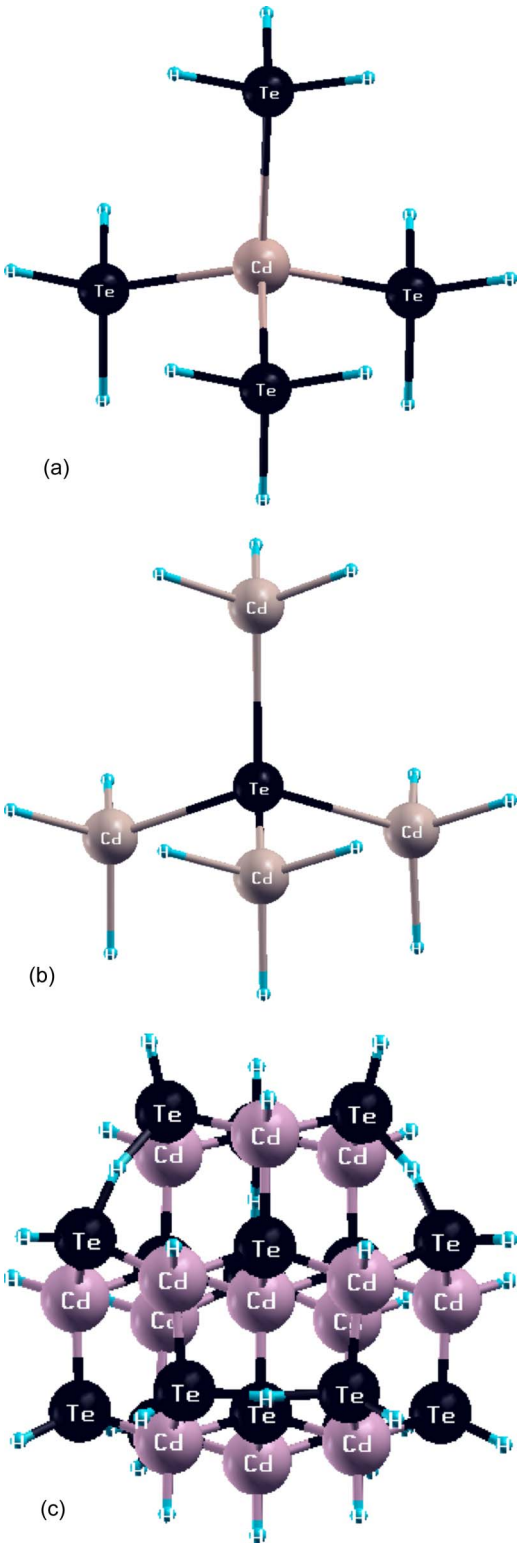

FIG. 13. (Color online) Relaxed geometries of (a) $Cd_1Te_4H^*_{12}$, (b) $Cd_4Te_1H^*_{12}$, and (c) $Cd_{13}Te_{16}H^*_{30}$. Black atoms are Te atoms and blue atoms are H^*.

An intriguing feature illustrated by the density of states (DOS) of these clusters is the presence of midgap states, i.e., states above HOMO in the gap region, due to the presence of dangling bonds in bare clusters, as shown in the Fig. 14(a).

Passivation has removed these midgap states resulting in opening of the gap,[37] as is visible in Fig. 14(b). Figure 15 compares the DOS for $Cd_{13}Te_{16}$ and $Cd_{13}Te_{16}H^*_{30}$ and quenching of midgap states on passivation is clearly visible. Passivation does not seem to affect geometry of small stoichiometric clusters but it does affect the electronic structure in agreement with experiment.

IV. CONCLUSION

The ground state geometries of Cd_nTe_n $(1 \leqslant n \leqslant 6)$ were calculated using *ab initio* DFT. The structures do not resemble that of the bulk phase as expected. Cd atoms tend to form a core group surrounded by the chalcogenide atoms because of the Coulomb repulsion of the lone pair of p electrons on Te. For Cd_nTe_n $(1 \leqslant n \leqslant 5)$, the planar geometry is found to be the lowest energy configuration as a linear Te-Cd-Te bond is preferred. But as the number of atoms increases further, higher coordination takes over and three dimensional structures result. Bonding in CdTe clusters is mostly covalent in nature with partial ionic character. The degree of ionicity decreases with increase in n. Nature of hybridization in HOMO and LUMO in these clusters is observed to be same as that of top of valence band and bottom of conduction band, respectively, in the bulk.

The relaxed structures of nonstoichiometric clusters Cd_mTe_n with $(m,n=1,4,13,16,19$ and $m \neq n)$, were obtained using *ab initio* DFT with the wave function projected to real space. The Te-rich clusters with Te atoms on the surface, are found to be more stable than the Cd-rich clusters. The symmetry of the cluster plays a vital role in determining its HOMO-LUMO gap. It was found that the Cd-rich clusters lose their initial T_d symmetry and attain a large HOMO-LUMO gap as compared to the Te-rich clusters.

Nonstoichiometric clusters were passivated using fictitious hydrogen atoms and are found to retain there T_d symmetry upon relaxation. Quenching of midgap states results in the opening of the band gap due to passivation. On the other hand, passivation has no effect on stoichiometric clusters. Stoichiometric clusters retain their structure and hence their symmetry. However, as in the case of non-stoichiometric clusters, in this case also the band gap opens up.

TABLE II. Summary of structural and electronic properties of relaxed $Cd_mTe_n(m \neq n)$ clusters. PG is the observed point group symmetry, BE is binding energy expressed in (eV/atom), l is average Cd-Te bond length in Å, θ is the Y-X-Y bond angle at the central atom X of the cluster, and E_g is the HOMO-LUMO gap in eV.

Clusters	PG	BE	l	θ	E_g
$Cd_1Te_4H_{12}^*$	T_d	2.39	2.82	109.47°	4.1
$Cd_4Te_1H_{12}^*$	T_d	2.39	2.83	109.47°	4.8
$Cd_{13}Te_{16}H^*_{30}$	T_d	2.30	2.84	109.47°	2.6

ACKNOWLEDGMENTS

We acknowledge financial support from the Department of Science and Technology, Government of India. We also thank IUCAA, Pune and Center for Modeling and Simulation, University of Pune for use of their computational facilities. We acknowledge D. G. Kanhere for fruitful discussion and J. R. Chelikowsky for the explanation and help in implementing the passivation.

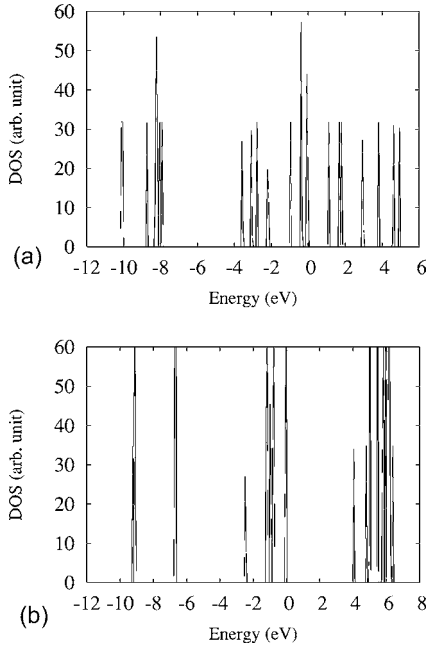

FIG. 14. Total DOS (a) Cd_1Te_4, (b) $Cd_1Te_4H^*_{12}$.

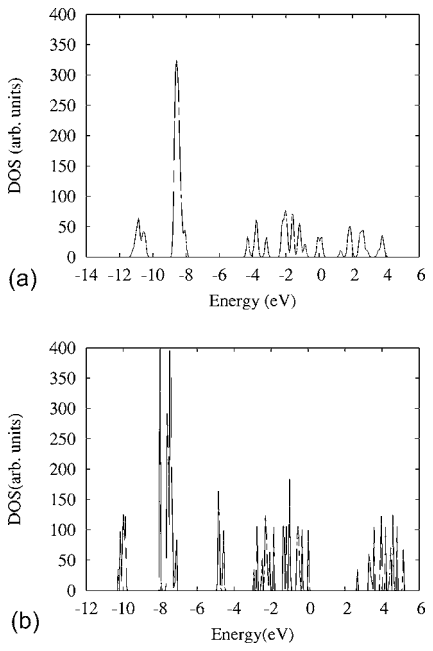

FIG. 15. Total DOS of (a) $Cd_{13}Te_{16}$ and (b) $Cd_{13}Te_{16}H^*_{30}$.

*Electronic address: skb@physics.unipune.ernet.in
†Author to whom correspondence should be addressed. Electronic address: anjali@physics.unipune.ernet.in

[1] V. L. Colvin, M. C. Schlamp and A. P. Alivisatos, Nature (London) **370**, 354 (1994); A. P. Alivisatos, J. Phys. Chem. **100**, 13226 (1996).
[2] S. Ögut, J. R. Chelikowsky, and S. G. Louie, Phys. Rev. Lett. **79**, 1770 (1997); I. Vasiliev, S. Ögut, and J. R. Chelikowsky, Phys. Rev. B **65**, 115416 (2002), and references therein.
[3] A. Shvartsberg (private communication).
[4] M. Gao, C. Lesser, S. Kirstein, H. Möhwald, A. L. Rogach, and H. Weller, J. Appl. Phys. **87**, 2297 (2000).
[5] J. Li *et al.*, Chem. Commun. (Cambridge) **8**, 982 (2004).
[6] N. W. Ashcroft and N. David Mermin, *Solid State Physics* (Holt-Saunders, Philadelphia, 1981).
[7] S. H. Wei and S. B. Zhang, Phys. Rev. B **62**, 6944 (2000).
[8] M. L. Cohen and J. R. Chelikowsky, in *Electronic Structure and Optical Properties of Semiconductors*, edited by M. Cardona (Springer-Verlag, Berlin, 1988).
[9] X. Q. Wang, S. J. Clark, and R. A. Abram, Phys. Rev. B **70**, 235328 (2004).
[10] V. S. Gurin, Int. J. Quantum Chem. **71**, 337 (1999); J.-O. Joswig *et al.*, J. Phys. Chem. B **104**, 2617 (2000); A. J. Williamson and A. Zunger, Phys. Rev. B **61**, 1978 (2000); J. M. Matxain, J. E. Fowler, and J. M. Ugalde, Phys. Rev. A **61**, 053201 (2000); J. M. Matxain, J. M. Mercero, J. E. Fowler, and J. M. Ugalde, *ibid.* **64**, 053201 (2001).
[11] J. Muilu and T. A. Pakkanen, Surf. Sci. **364**, 439 (1996).
[12] E. Spano, S. Hamad, and C. R. Catlow, J. Phys. Chem. **13**, 10337 (2003).
[13] V. Albe, C. Jouanin, and D. Bertho, J. Cryst. Growth **184/185**, 388 (1998); S. Pokrant and K. B. Whaley, Eur. Phys. J. D **6**, 255 (1999).
[14] L. W. Wang and A. Zunger, Phys. Rev. B **53**, 9579 (1996).
[15] K. Shirashi, J. Phys. Soc. Jpn. **59**, 3455 (1990).
[16] L. W. Wang and J. Li, Phys. Rev. B **69**, 153302 (1994).
[17] X. Huang, Eric Lindgren, and J. R. Chelikowsky, Phys. Rev. B **71**, 165328 (2005).
[18] P. Hohenberg and W. Kohn, Phys. Rev. **136**, B864 (1964); W. Kohn and L. J. Sham, Phys. Rev. **140**, A1133 (1965).
[19] P. E. Blöchl, Phys. Rev. B **50**, 17953 (1994); G. Kresse and D. Joubert, *ibid.* **59**, 1758 (1999).
[20] G. Kresse and J. Furthmuller, Phys. Rev. B **54**, 11169 (1996); Comput. Mater. Sci. **6**, 15 (1996).
[21] A. Pasquarello, K. Laasonen, R. Car, C. Lee, and D. Vanderbilt, Phys. Rev. Lett. **69**, 1982 (1992); K. Laasonen, A. Pasquarello, R. Car, C. Lee, and D. Vanderbilt, Phys. Rev. B **47**, 10142 (1993).
[22] O. Gunnarsson and R. Jones, in *Local Density Approximations in Quantum Chemistry and Solid State Theory*, edited by J. P. Dahl and J. Avery (Plenum, New York, 1983), pp. 229.
[23] J. P. Perdew, K. Burke, and M. Ernzerhof, Phys. Rev. Lett. **77**, 3865 (1996).
[24] J. P. Perdew, *Electronic Structure of Solids '91*, edited by P. Ziesche and H. Eschrig (Akademie Verlag, Berlin, 1991), pp. 11; J. P. Perdew and Y. Wang, Phys. Rev. B **45**, 13244 (1992).
[25] N. Kosugi, J. Comput. Phys. **55**, 426 (1984).
[26] M. C. Troparevsky and J. R. Chelikowsky, J. Chem. Phys. **114**, 943 (2001).
[27] S.-H. Wei and A. Zunger, Phys. Rev. B **37**, 8958 (1988); J. Cryst. Growth **86**, 1 (1988).
[28] Some of our results on stoichiometric ZnS clusters using PBE and PAW are used (unpublished).
[29] J. Zhao, Phys. Rev. A **64**, 043204 (2001).
[30] D. Vogel, P. Krüger, and J. Pollmann, Surf. Sci. **402–404**, 774 (1998).
[31] Our results on Te clusters using PBE and PAW are used (unpublished).
[32] GAUSSIAN 03, Revision B.03, M. J. Frisch *et al.* (Gaussian, Inc., Pittsburgh, PA, 2003).
[33] P. Blaha, K. Schwarz, P. Sorantin, and S. B. Trickey, Comput. Phys. Commun. **59**, 399 (1990).
[34] T. Nanba, Y. Nodake, M. Muneyasu, G. P. Williams, and S. Hayashi, J. Phys. Soc. Jpn. **66**, 1526 (1997); R. Banerjee, R. Jayakrishnan, and P. Ayyub, J. Phys.: Condens. Matter **12**, 10647 (2000).
[35] G. M. Dalpian, M. L. Tiago, M. L. Puerto, and J. R. Chelikowsky, Nano Lett. **6**, 501 (2006).
[36] A. Puzder, A. J. Williamson, F. Gygi, and G. Galli, Phys. Rev. Lett. **92**, 217401 (2004).
[37] Sameer Sapra and D. D. Sarma, Phys. Rev. B **69**, 125304 (2004).